

# DoDo-Code: a Deep Levenshtein Distance Embedding-based Code for IDS Channel and DNA Storage

Alan J.X. Guo\*, Sihan Sun, Xiang Wei, Mengyi Wei, Xin Chen

December 21, 2023

## Abstract

Recently, DNA storage has emerged as a promising data storage solution, offering significant advantages in storage density, maintenance cost efficiency, and parallel replication capability. Mathematically, the DNA storage pipeline can be viewed as an insertion, deletion, and substitution (IDS) channel. Because of the mathematical terra incognita of the Levenshtein distance, designing an IDS-correcting code is still a challenge. In this paper, we propose an innovative approach that utilizes deep Levenshtein distance embedding to bypass these mathematical challenges. By representing the Levenshtein distance between two sequences as a conventional distance between their corresponding embedding vectors, the inherent structural property of Levenshtein distance is revealed in the friendly embedding space. Leveraging this embedding space, we introduce the DoDo-Code, an IDS-correcting code that incorporates deep embedding of Levenshtein distance, deep embedding-based codeword search, and deep embedding-based segment correcting. To address the requirements of DNA storage, we also present a preliminary algorithm for long sequence decoding. As far as we know, the DoDo-Code is the first IDS-correcting code designed using plausible deep learning methodologies, potentially paving the way for a new direction in error-correcting code research. It is also the first IDS code that exhibits characteristics of being ‘optimal’ in terms of redundancy, significantly outperforming the mainstream IDS-correcting codes of the Varshamov-Tenengolts code family in code rate.

## 1 Introduction

In recent years, DNA storage has emerged as a promising data storage approach [1–8]. This method offers significant advantages over conventional storage techniques, including its remarkable storage density, low maintenance cost, and efficient parallel replication capabilities [9].

A typical DNA storage pipeline includes the following key steps [6]. Firstly, the binary information is encoded into a series of strings, called *references*, on the alphabet  $\{A, T, G, C\}$ . Subsequently, the DNA molecules are synthesized according to these references. Later the DNA molecules are amplified and preserved. To retrieve the stored information, the DNA molecules are sequenced into another bucket of strings, referred to as *reads*. These reads are then clustered to recover the corresponding references, which in turn are employed to decode the original binary information.

Because of the biochemical procedures involved in the pipeline, the reads obtained from references are often affected by base insertions, deletions, or substitutions (IDS) [10]. In the early stages of DNA storage research, established codes like the Reed-Solomon (RS) code [3], the fountain code [4], and the low-density parity check (LDPC) [11] were employed. More recently, heuristic codes adapted to the IDS channel have incorporated synchronization markers [12, 13] or watermarks [14] to rectify synchronization errors or generate implicitly disjoint segments. Noteworthy examples include codes such as those presented in [15–17]. In contrast, the HEDGES [18] does not explicitly use a synchronization marker. Their encoding procedure involves position indexing. Several mathematical approaches have utilized intricate mathematical and combinatorial techniques to design synchronization error-correcting codes, including [19–24]. Most of these works use Varshamov-Tenengolts (VT) code as their backbone algorithm.

Many of these segmented error-correcting codes, designed to handle a single edit error in each segment, pursue order-optimal redundancy of  $\log N + o(\log N)$  bits, where  $N$  is the length of codewords. Several abovementioned codes achieve order-optimality, while others are close to this mark. In [23], a code of length

---

\*A.J.G., S.S., X.W., M.W., and X.C. are with the Center for Applied Mathematics, Tianjin University, China. This work was supported by the National Key Research and Development Program of China under Grant 2020YFA0712100. (CONTACT: jiaxiang.guo@tju.edu.cn)

$n$  which is capable of correcting a single edit error over 4-ary alphabet with a redundancy of  $\log n + O(\log \log n)$  bits is introduced. The code of least redundancy bits till now is proposed in [25], the researcher presented an improved method with redundancy bits of  $\log n + \log \log n + 7 + o(1)$ , which reduces the redundancy by 6 bits compared to the original code in [23]. Despite the order-optimality of these codes, applying them in the field of DNA storage presents a dilemma. Taking the state-of-the-art code proposed in [25] for example. To generate an IDS-correcting reference of length  $n_0 > 100$  in a DNA storage pipeline, one could either use a code of length  $n_0$  to produce the reference in one step or concatenate  $n_0/n$  codeword segments of length  $n \ll n_0$  to form the reference. However, both of these paths are impractical. The primary reasons are:

- For the one-step generation of the reference sequence, it can only correct one single edit error in the entire sequence, which is overly optimistic for DNA storage applications. Multi-edit errors in a single read are common in a DNA storage pipeline [10].
- Regarding the concatenation of codewords of small length  $n$ , the resulting reference can correct multi-edit errors to some extent. However, the constant term in the required redundancy bits dominates, leading to a low code rate. As suggested in Figure 4, even the state-of-the-art code [25], which is order-optimal, exhibits a impractical low coderate when  $n$  is small.

To tackle the challenge of designing mathematically proven IDS-correcting codes for the DNA storage pipeline, we focus on constructing a code using a more fundamental approach. Let's revisit the basics of classical codes [26]. Given a code  $C$ , which is a collection of codewords, its minimum distance is defined as follows:

$$d(C) = \min\{d(u, v) : u, v \in C, u \neq v\}. \quad (1)$$

Once a code  $C$  with a minimum distance of  $d$  is constructed, a bounded distance decoder (BDD) with decoding radius  $r = \lfloor \frac{d-1}{2} \rfloor$  is straightforward. This BDD decodes a given word  $x$  to the corresponding codeword  $y$  such that  $d(x, y) \leq r$ . The Levenshtein distance [20] is a pivotal concept in codes for the IDS channel. This distance is defined as the minimum number of insertions, deletions, and substitutions required to transform one sequence into another. Building upon the principles of BDD, we are going to develop a simple code  $C(n)$  of fixed length  $n$ . Its codewords are designed to maintain a mutual Levenshtein distance of 3, thereby endowing the code with the capacity to correct one single IDS error within each codeword.

However, the construction of such a code faces three significant challenges. Firstly, the sizes of Levenshtein balls, which represent the set of a sequence and its neighboring sequences within a Levenshtein distance of  $r$ , exhibit a lack of homogeneity [27, 28]. Researchers want to select sequences with small Levenshtein balls as the codewords to enhance the code rate. However, a clear depiction of Levenshtein balls is still absent [27, 28], and an algorithm surpassing random codeword selection has not yet been published to the best of our knowledge. Secondly, the computational complexity of the BDD based on the Levenshtein distance is substantial. The complexity of computing the Levenshtein distance is at least  $O(n^{2-\epsilon}), \forall \epsilon > 0$  [29, 30], unless the strong exponential time hypothesis is false. Additionally, most of the existing searching algorithms, primarily designed for conventional distance [31], are inapplicable to the Levenshtein distance. Thirdly, to generate an encoded long reference, an effective strategy is concatenating the codewords of  $C(n)$  to reach the desired reference length. Retrieved from the DNA storage pipeline, the reads may carry synchronization errors from the references. Simply splitting the reads into segments of length  $n$  during the decoding process can lead to synchronization mismatches and result in failures.

To address these challenges, we introduce a novel bounded distance code, which leverages the deep embedding of the Levenshtein distance, and call it DoDo-Code. The proposed DoDo-Code uses a comprehensive approach includes the following key procedures: deep embedding of Levenshtein distance; deep embedding-based greedy search of codewords, depicted in Figure 1; deep embedding-based segment correcting, illustrated in Figure 2; long sequence decoding utilizing the depth-first search (DFS) [32], introduced in Figure 3. In the following text, we offer a concise introduction to these procedures.

Considering the complexity of calculating the Levenshtein distance, researchers have explored mapping sequences into embedding vectors, and use a conventional distance between these vectors to approximate the Levenshtein distance [33, 34]. Recently, deep learning techniques have been employed for Levenshtein distance embedding and achieved remarkable performance across various works [35–39]. Mathematically, given two sequences  $\mathbf{s}, \mathbf{t}$ , the embedding function  $f(\cdot)$  maps the two sequences to the embedding vector  $\mathbf{u} = f(\mathbf{s}), \mathbf{v} = f(\mathbf{t})$  individually. Researchers utilize a conventional distance, for example the Euclidean distance, between the embedding vectors  $\hat{d} = \|\mathbf{u} - \mathbf{v}\|_2$  to approximate the Levenshtein distance  $\Delta_L(\mathbf{s}, \mathbf{t})$  between the original sequences  $\mathbf{s}$  and  $\mathbf{t}$ . From a broader perspective, we find that these embeddings not only accelerate the Levenshtein distance estimation, but also offer a way to analyze the properties and structures of the Levenshtein distance. The embedding vectors carry the properties of their original sequences from

the Levenshtein distance domain, and present these properties within a more friendly embedding vector space. For example, in the vector space, the embedding vectors of sequences within a Levenshtein ball should naturally exhibit a tight clustering. In this study, we adopt the embedding framework from [38, 39], and modify it to make the embedding model focus more on small Levenshtein distances.

To construct the code  $C(n)$ , a straightforward approach is repeating the following procedure: randomly selecting a sequence from a candidate set (initially consists of all possible sequences  $A(n) = \{A, T, G, C\}^n$ ), and then filtering out the neighboring sequences of the chosen one from this set. This strategy, however, neglects the inherent Levenshtein property of these sequences. In this work, we introduce an alternative approach. Firstly, a statistical distribution is estimated on the embedding vectors  $f(A(n))$ . Subsequently, the sequence from the candidate set whose embedding vector possesses the lowest probability density function (PDF) value is chosen as a codeword. Finally, the candidate set is updated by filtering out the Levenshtein ball, and this selection is repeated until the candidate set becomes empty. The entire procedure for the greedy selection of codewords is illustrated in Figure 1.

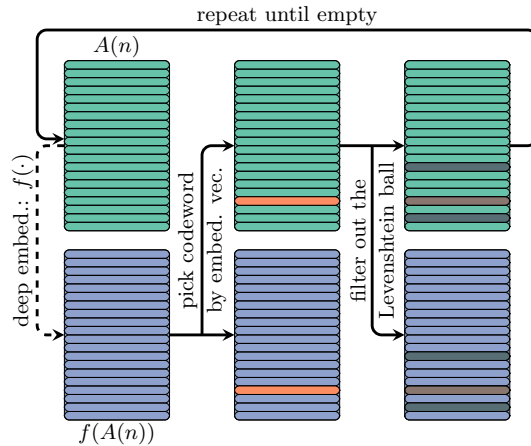


Figure 1: Flowchart illustrating the deep embedding-based greedy search of codewords. The initial candidate set consists of all possible sequences  $A(n) = \{A, T, G, C\}^n$ . During each iteration, the codeword is selected as the sequence whose embedding vector has the lowest PDF value. The selected codeword and its neighboring sequences are filtered out from the candidate set before the next iteration.

In Figure 2, we outline the procedure by which a corrupted codeword is corrected by the proposed DoDo-Code. If we designate a corrupted codeword as a segment, a plausible method for segment correcting is calculating the Levenshtein distance between this segment and all the codewords, and then selecting the codeword with the minimal distance as the correction. However, this brute-force approach costs significant computational complexity, scaling up to  $O(n^2|C(n)|)$ . It is worth noting that the cardinality of the code  $|C(n)|$  grows fast as  $n$  increases in the experiments. In this work, we capitalize on the deep embedding vectors and their conventional distances. Specifically, we construct a K-dimension tree (K-d tree) [40] by the embedding vectors  $f(C(n))$  corresponding to the codewords. Subsequently, the embedding vector of the segment is utilized to query its nearest neighbors within this K-d tree, thereby confirming the nearest codewords to this segment. Notably, the querying operation from the K-d tree average costs  $O(\log |C(n)|)$  in complexity [41], which is a substantial reduction compared to the aforementioned brute-force search.

In the DNA storage pipeline, the lengths of both references and reads typically extend beyond 100nt. Implementing a greedy search for codewords of the same length as the reference is infeasible in complexity. Additionally, a reference capable of correcting only one edit error lacks applicability in the context of DNA storage. Therefore, we need to concatenate multiple codewords that carry information to generate an encoded reference. However, during the decoding of the retrieved read sequence, the occurrence of synchronization errors may cause segment misalignments. Since the proposed code allows for one edit error in each segment, we attempt to correct the three segments of lengths  $n-1, n$ , and  $n+1$  originating from the same position of the read. By recursive attempts of segment correctings on the undecoded part of the read, the decoding process, as illustrated in Figure 3, generates a ternary tree. The successful correction of the read is represented by one of the leaf nodes. The experiments demonstrate that the concerns about the complexity of such a ternary tree are unnecessary. This is primarily due to the fact that a synchronization mismatch results in a bucket of errors during subsequent decoding attempts, thereby enabling an early termination of the incorrect decoding branches.

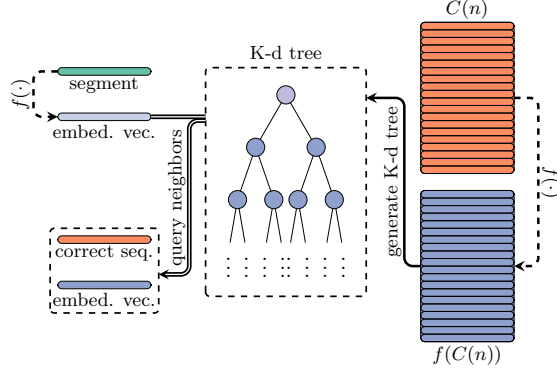


Figure 2: Flowchart for the deep embedding-based segment correcting. A K-d tree is constructed using the embedding vectors  $f(C(n))$  of all the codewords. The embedding vector of a segment is used to query the K-d tree for its neighboring sequences. By calculating the Levenshtein distances between the segment and the retrieved neighbors, the corrected codeword is identified.

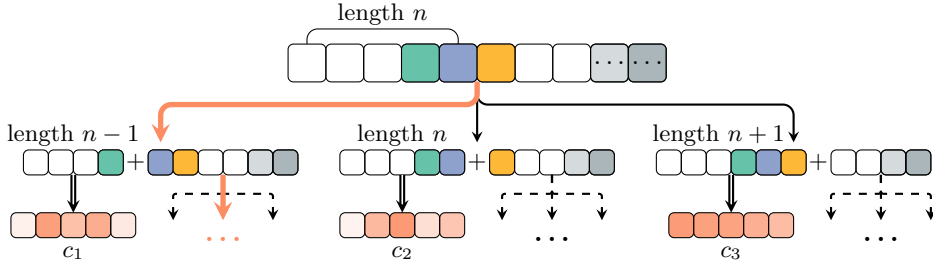


Figure 3: Flowchart illustrating the DFS-based long sequence decoding. The decoding process recursively attempts to decode segments of lengths  $n - 1$ ,  $n$ , and  $n + 1$  within the undecoded sequence. A ternary tree is constructed to represent these recursive steps, and finally, a leaf node with the minimal prediction distance represents the decoded sequence.

As a result, the proposed DoDo-Code offers a solution for IDS channel codes and DNA storage, excelling in the following aspects. Taking advantage of the deep embedding-based greedy search of codewords, the proposed DoDo-Code achieves a code rate that surpasses the state-of-the-art and shows optimality when code length  $n$  is small. Using the deep embedding-based segment correcting method, the computational complexity is effectively reduced to  $O(1)$  of the encoder and  $O(n)$  of the decoder. And one edit operation corrupted codewords can be firmly corrected. Employing the DFS-based long sequence decoding algorithm, the long sequence decoding reports an error rate below 0.5%. This residual error can be eliminated by leveraging an outer RS code of 2% error-correcting code (ECC) symbols. The concatenated code of DoDo-Code and RS code has an overall code rate up to 67.5%. To the best of our knowledge, the DoDo-Code is the first IDS code designed by deep learning methodologies and the first IDS code that seems to be ‘optimal’ when the code length is small.

## 2 Results

### 2.1 Code rate and optimality

The utilization of the deep embedding-based greedy search yields an augmented count of codewords, thereby promoting the overall code rate. As suggested in Table 1, the cardinality of the code is enlarged by the proposed greedy search compared to random codeword selection. This is of our research interest, because a larger code cardinality directly translates to lower redundant and a higher code rate. Moreover, we observe that the augmentation in codeword count becomes more pronounced when the codeword length  $n$  increases. For instance, when  $n = 11$ , the deep embedding-based greedy search identifies 16.8% more codewords compared to the approach of random codeword selection.

By selecting the code with the maximum cardinality from among 10 runs of the computational experi-

Table 1: The cardinality of constructed code. The results are reported as the mean value and maximum value over 10 runs of the experiments. The method “Rand” stands for random codeword selection, while the method “DEGS” stands for the proposed deep embedding-based greedy search.

	Method	$n = 7$	$n = 8$	$n = 9$	$n = 10$	$n = 11$
avg.	Rand	251.5	813.2	2694.0	9091.7	31071.9
	DEGS	267.5	884.8	3001.6	10325.4	35973.1
	$\Delta$	+6.4%	+8.8%	+11.4%	+13.6%	+15.8%
max.	Rand	259	820	2717	9124	31142
	DEGS	275	900	3011	10414	36368
	$\Delta$	+6.2%	+9.8%	+10.8%	+14.1%	+16.8%

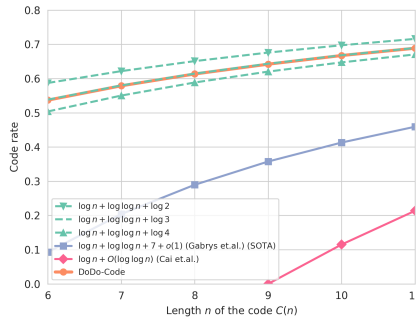


Figure 4: The code rate of code searched by deep embedding-based greedy search strategy, reported as the best in 10 runs. Comparison methods are the-state-of-art approaches in [23, 25]. We also plot the code rates corresponding to order-optimal redundancies of  $\log n + \log \log n + 1$ ,  $\log n + \log \log n + \log 3$ , and  $\log n + \log \log n + 2$ . These levels of redundancies are not achieved by any codes before our work.

ments, we calculate the corresponding code rate using the formula:

$$r(n) = \frac{\log_4 |C(n)|}{n}, \quad (2)$$

and visualize them against the code length in Figure 4. For comparison, we present the code rates of the approach introduced in [23] which is order-optimal with redundancy of  $\log n + O(\log \log n)$  bits, as well as the state-of-the-art code rates from [25] which is also order-optimal using  $\log n + \log \log n + 7 + o(1)$  redundancy bits. Additionally, we draw the code rates corresponding to the order-optimal redundancies of  $\log n + \log \log n + 1$ ,  $\log n + \log \log n + \log 3$ , and  $\log n + \log \log n + 2$ . It’s worth noting that for small code lengths  $n$ , no existing 4-ary code achieves these levels of redundancies.

The figure clearly exhibits a trend of increasing code rates with longer codeword lengths  $n$ . Remarkably, for  $n = 11$ , the code rate reaches 68.9%. Even with the incorporation of an outer RS code with 2% ECC symbols to correct failures in long sequence decoding discussed in the following text, the overall code rate remains above 67.5%. This demonstrates that our code offers a solution with less than 50% redundancy of nucleotide bases for DNA storage. In comparison to existing state-of-the-art works [23, 25], the DoDo-Code has a significantly higher code rate. Furthermore, when compared to the order-optimal redundancies of  $\log n + \log \log n + 1$ ,  $\log n + \log \log n + \log 3$ , and  $\log n + \log \log n + 2$ , the code rate curve of DoDo-Code lies between  $\log n + \log \log n + 1$  and  $\log n + \log \log n + 2$  and overlaps the curve of  $\log n + \log \log n + \log 3$  exactly. We would like to claim that the proposed DoDo-Code is approximately order-optimal using  $\log n + \log \log n + \log 3$  redundancy bits. However, this assertion lacks theoretical proof in this study.

It’s interesting to note that  $\log n + \log \log n + \log 3$  can be reformulated as  $\log 3n + \log \log n$ , which provides some insight into the close alignment between the code rate curves of DoDo-Code and  $\log n + \log \log n + \log 3$ . As mentioned above, correcting one bit flip in  $N$  bits requires at least  $\log N$  redundancy bits for information to identify the error position. In the context of 4-ary code, correcting a substitution in  $n$  bases requires information on both the error position and the substituted letter, which could be any of the other three letters. As a result, a minimum of  $\log 3n$  redundancy bits are required. From this, it may be inferred that  $\log 3n + \log \log n$  is perhaps the least redundancy we can reach. Based on the computational experiments, we may raise the following conjecture:

**Conjecture 1.** *There exists a 4-ary code of length  $n$  that corrects one edit error using  $\log 3n + \log \log n$  redundancy bits.*

Maybe some mathematicians could have further research leveraging combinatorial or probability methods.

## 2.2 Success rate and time complexity of segment correcting

The proposed deep embedding-based segment correcting method is both efficient and reliable. Constructed by filtering out the Levenshtein balls, the resulting code ensures that codewords maintain a minimum mutual Levenshtein distance of 3. Hence, one single edit error in a codeword can be confidently corrected by the BDD. The deep embedding-based segment correcting utilizes a tree search on the embedding vectors to reduce time complexity. As suggested in Figure 5, the proposed method leads to a substantial reduction in time complexity compared to the brute-force approach, which corrects the segment by brutally searching for the codeword with the minimal Levenshtein distance. However, the deep embedding of the Levenshtein distance introduces approximation error, affecting the reliability of the nearest neighbor achieved from the tree search. An effective solution is increasing the number  $k$  of searched neighbors, and then performing a double confirmation by Levenshtein distance. As indicated in Table 2, the number of failed corrections notably decreases when searching for  $k = 2$  neighbors. Further increasing the searched neighborhood to  $k = 4$ , the number of failed corrections is 0 in correcting 100,000 modified codewords. Importantly, the increase of time cost is minimal by raising  $k$  from 1 to 5, as shown in Figure 5.

Table 2: Number of failed segment correctings in 100,000 tries by using tree search. The segments are obtained by randomly one edit modification on the codewords.  $k$  is the number of neighbors queried in the tree search.

	$n = 7$	$n = 8$	$n = 9$	$n = 10$	$n = 11$
$k = 1$	328	389	454	779	841
$k = 2$	0	5	4	4	11
$k = 3$	0	0	2	0	0
$k = 4$	0	0	0	0	0

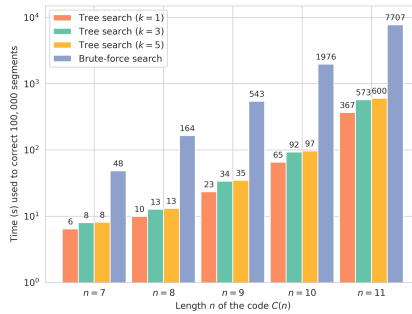


Figure 5: The time used to correct 100,000 segments. The segments are obtained by randomly one edit modification on the codewords.  $k$  is the number of neighbors in the tree search. The brute-force search calculates the Levenshtein distance between the segment and codewords until the finding of a 1-distance codeword. The  $y$ -axis is in log scale.

## 2.3 Error rates of long sequence decoding

In order to match the reference length in DNA storage, encoded codeword segments are concatenated. However, the retrieved reads may lose information about the segment boundaries due to synchronization errors. As mentioned above, we introduce a preliminary DFS-based long sequence decoding. The error rates resulting from the proposed DFS decoding are presented in Figure 6. Given a reference sequence of approximately 150nt in length, the read sequence is generated by introducing a 1% chance of edit operation, which has equal probabilities of insertion, deletion, and substitution, at each nucleotide position of the reference. To evaluate the proposed method, two metrics are employed: the sequence error rate (SeqER), which denotes the ratio of unsuccessfully decoded reads among all the decoded reads, and the segment error rate (SegER),

which represents the ratio of failed segments among all the segments concatenated to form the references. As shown in Figure 6, the SeqER is about 5% and the SegER is around 0.4%. Recall that the proposed code is designed to be 3-Levenshtein distance separable, implying that the code may fail to correct more than one edit error in the same segment. To investigate the potential causes of decoding failures in long sequences, we conduct experiments by limiting the edit operations to prevent multiple edit errors in the same segment of the reads. These results are denoted as SeqER\* and SegER\* in Figure 6. By comparing the SeqER (resp. SegER) with SeqER\* (resp. SegER\*), we can infer that multiple edit errors in the same segment is the main reason for long sequence decoding failures.

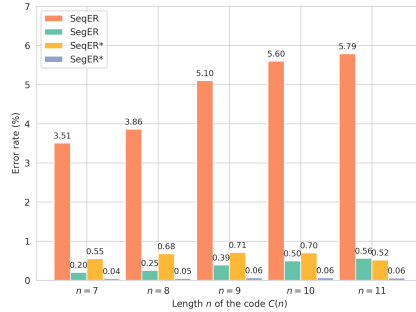


Figure 6: Error rates of long sequence correcting. The numbers are reported over 10,000 long sequence decoding. Each sequence is corrupted by 1% chance of edit operation on each position of nucleotide. SeqER\* and SegER\* are the error rates on sequences that forbid multiple edit errors in the same segment.

The average count of failed segments in each unsuccessful long sequence decoding is reported in Table 3. It should be noted that every unsuccessful long sequence decoding carries at least one failed segment. Therefore, the results in Table 3 indicate that the proposed DFS decoding possesses the capability to successfully decode segments after failed segments. This also demonstrates that the proposed decoding approach can restore the segment boundaries after encountering a failed segment.

Table 3: The average number of failed segments in each failed long sequence decoding.

	$n = 7$	$n = 8$	$n = 9$	$n = 10$	$n = 11$
# failed seg.	1.22	1.17	1.22	1.34	1.27

As observed in Figure 6, the SegER ranges between approximately 0.3% and 0.6%. Using an outer ECC, such as an RS code [42] over a Galois field, can effectively correct such errors. However, by the proposed DoDo-Code, the encoded information is represented as numbers from 0 to  $|C(n)| - 1$ , which may not be compatible with a Galois field. Slightly reducing the number of codewords addresses this issue. Let  $p$  be the largest prime number less or equal to  $|C(n)|$ , which is not far from  $|C(n)|$  based on the prime number theorem [43]. By using the first  $p$  codewords of  $C(n)$  and implementing an outer RS code over  $GF(p)$ , an end-to-end code that corrects IDS errors in long sequences is achieved. A practical Python implementation of the RS code over  $GF(p)$  can be found in [44]. Taking the code  $C(n = 10)$  as an example, it has cardinality  $|C(10)| = 10414$  as shown in Table 1, and the nearest prime number below  $|C(10)|$  is  $p = 10399$ . Thus, the first  $p = 10399$  codewords from  $C(10)$  are employed as the inner code, while the corresponding outer code is selected as the RS code over  $GF(p = 10399)$ . Various ratios of ECC symbols ranging from 0 to 3% are explored across different code lengths, including  $n = 9$ ,  $n = 10$ , and  $n = 11$ . The results are presented in Figure 7. It is suggested that the SegER decreases as the number of ECC symbols increases, and using an outer code with 2% or more ECC symbols can effectively eliminate the errors.

### 3 Details of the proposed method

#### 3.1 Deep embedding of Levenshtein distance

In this work, we follow the framework proposed in [38, 39], and modify the optimization target to make the embedding model focus on small Levenshtein distances.

Let  $\mathbf{s}$  and  $\mathbf{t}$  denote two sequences of length  $n$  on the alphabet  $\{A, T, G, C\}$ , and let  $d = \Delta_L(\mathbf{s}, \mathbf{t})$  represent the groundtruth Levenshtein distance between them. Our task is to identify an embedding function  $f(\cdot)$ ,

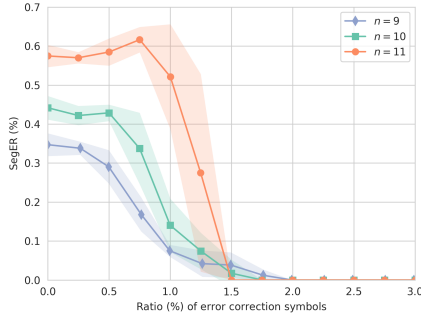


Figure 7: The SegER after applying an outer RS code. The curves are drawn by the mean value and the standard deviation of SegER over 5 runs. The concatenated code for  $n = 9$  is  $C(9)$  and RS code over  $GF(3011)$ ; the concatenated code for  $n = 10$  is  $C(10)$  and RS code over  $GF(10399)$ ; and the concatenated code for  $n = 11$  is  $C(11)$  and RS code over  $GF(36353)$ . The  $x$ -axis is the ratio of ECC symbols in the RS code.

such that the mapped embedding vectors  $\mathbf{u} = f(\mathbf{s})$  and  $\mathbf{v} = f(\mathbf{t})$  have a conventional distance  $\hat{d} = \Delta(\mathbf{u}, \mathbf{v})$  close to the groundtruth Levenshtein distance  $d$ . Let  $f(\cdot; \theta)$  be a trainable deep embedding model, which is implemented as a model with 10 1D-CNN [45] layers and one final batch normalization [46] in this study. The notation  $\theta$  is for the learnable parameters of the deep model. The training of  $f(\cdot; \theta)$  can be expressed as an optimization of:

$$\hat{\theta} = \arg \min_{\theta} \sum \mathcal{L}(d, \hat{d}; \theta) = \arg \min_{\theta} \sum \mathcal{L}(d, \Delta(f(\mathbf{s}; \theta), f(\mathbf{t}; \theta))), \quad (3)$$

where the function  $\mathcal{L}(\cdot, \cdot)$  is a predefined loss function that measures the disparity between the predicted distance and the groundtruth distance. By optimizing Equation (3), the parameters of the embedding model are learned and denoted as  $\hat{\theta}$ , and the optimized deep embedding model  $f(\cdot; \hat{\theta})$  is capable of mapping sequences to their corresponding embedding vectors. This model configuration is often referred to as a Siamese neural network [47]. A brief illustration of the utilized Siamese neural network is presented in Figure 8.

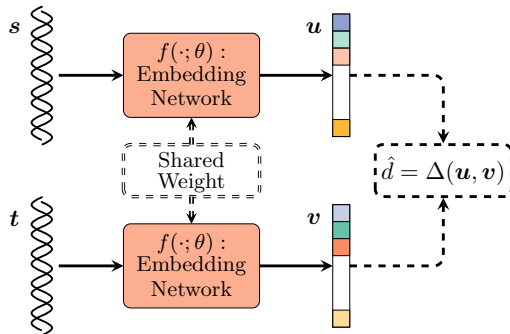


Figure 8: Siamese neural network. Given two sequences  $\mathbf{s}, \mathbf{t}$ , the network employs two branches of the embedding model, sharing the same parameters, to map them to their respective embedding vectors  $\mathbf{u}, \mathbf{v}$ . The approximate distance is calculated as a conventional distance between  $\mathbf{u}$  and  $\mathbf{v}$ . The model is trained by optimizing a predefined loss function that measures the disparity between the predicted distance  $\hat{d}$  and the groundtruth Levenshtein distance  $d$ .

We employ the squared Euclidean distance between the embedding vectors as the approximation of the groundtruth Levenshtein distance. The squared Euclidean distance is defined as:

$$\hat{d} = \Delta(\mathbf{u}, \mathbf{v}) = \sum_i (u_i - v_i)^2. \quad (4)$$

Although the squared Euclidean distance is not a true distance metric, its effectiveness has been validated in [38, 39]. Moreover, it is the square of the Euclidean distance and therefore compatible with the K-d tree employed in this work. The loss function of Levenshtein distance prediction was designed to provide a



global approximation of the Levenshtein distance. However, since we focus more on the Levenshtein balls and neighboring sequences, we modify the loss function to emphasize the prediction of small Levenshtein distances. Specifically, the model is trained to provide precise prediction for 1 Levenshtein distance and ensure that the predicted distance is greater than 2 when the groundtruth distance is greater or equal to 2. The revised loss function is defined as follows:

$$\tilde{\mathcal{L}}(d, \hat{d}) = \begin{cases} \mathcal{L}(d, \hat{d}) & \text{if } d = 1; \\ \mathbb{1}_{\hat{d} < 2} \cdot \mathcal{L}(2, \hat{d}) & \text{if } d \geq 2, \end{cases} \quad (5)$$

where  $\mathbb{1}_{\hat{d} < 2}$  is the indicator function that evaluates to 1 when  $\hat{d} < 2$ .

For the sake of brevity, we will use  $f(\cdot)$  to represent the learned embedding function  $f(\cdot; \hat{\theta})$  in the subsequent discussion.

### 3.2 Deep embedding-based greedy search of codewords

As shown in Figure 1, the code construction procedure begins by initializing the candidate set as the collection of all possible sequences, denoted as  $A(n) = \{A, T, G, C\}^n$  with length  $n$ . In the subsequent steps, the sequence from the candidate set is iteratively chosen as the codeword, and the codeword and its neighboring sequences within a Levenshtein ball of radius 2 are simultaneously removed from the candidate set. This iterative process of codeword selection continues until the candidate set is exhausted.

The selection criterion for choosing codewords from the candidate set is the key part of the search algorithm. Maximizing the code’s cardinality is desirable to enhance the code rate. In a greedy search approach, the codewords with fewer neighbors should be selected in advance. However, only the minimum, maximum, and average sizes of Levenshtein balls with radius one are studied in existing works [27,28], which is insufficient to establish an applicable criterion for codeword selection.

Fortunately, the deep embedding of Levenshtein distance builds a connection between the structural characteristics of Levenshtein distances and the distribution properties of the embedding vectors. Through this deep embedding, it becomes possible to depict the Levenshtein ball of a given codeword  $\mathbf{s}$  by the Euclidean ball centered at the embedding vector  $\mathbf{u} = f(\mathbf{s})$ . As mentioned above, the embedding network employs a final batch normalization, which forces the embedding vector  $\mathbf{u}$  to follow a multivariate normal distribution  $N(\mathbf{0}, \Sigma)$  with a mean vector  $\mathbf{0}$  and a covariance matrix  $\Sigma$ . Let  $m$  denote the dimension of the random vector, the PDF of  $N(\mathbf{0}, \Sigma)$  is formulated as

$$p(\mathbf{x}) = (2\pi)^{-\frac{m}{2}} |\Sigma|^{-\frac{1}{2}} \exp\left(-\frac{1}{2} \mathbf{x}^T \Sigma^{-1} \mathbf{x}\right). \quad (6)$$

The covariance matrix  $\Sigma$  is easy to estimate with all the possible embedding vectors  $f(A(n))$ . With the estimated covariance matrix  $\hat{\Sigma}$ , the PDF of  $N(\mathbf{0}, \hat{\Sigma})$  for each embedding vector can be calculated using Equation (6). To achieve the goal of selecting codewords with fewer neighbors, an effective criterion can be expressed in the embedding space as the sequence whose embedding vector has the lowest PDF value should be chosen as the codeword. A step further, by making some simplifications to Equation (6), an embedding vector  $\mathbf{u}$  should be selected if  $\mathbf{u}^T \Sigma^{-1} \mathbf{u}$  is the maximum over the candidate set.

As illustrated in Table 1, this proposed criterion results in up to 16.8% more codewords for a code length of  $n = 11$ .

### 3.3 Deep embedding-based segment correcting

As mentioned above, the selected codewords maintain a minimum mutual Levenshtein distance of 3. Therefore, a segment of codeword corrupted by one edit operation is fully correctable by using BDD algorithm. However, employing a brute-force approach to search for the nearest codeword from a given segment costs a substantial time complexity of  $O(n^2|C(n)|)$ . Since the cardinality of the code  $|C(n)|$  grows fast with increasing code length  $n$ , as demonstrated in Table 1, the complexity of  $O(n^2|C(n)|)$  becomes impractical when  $n$  is large.

Thanks to the utilization of the deep embedding model, we can leverage the embedding vectors to efficiently search for neighboring codewords of a given segment. The K-d tree, a classical data structure, provides a fast look-up method for the nearest neighbors of a given vector. As illustrated in Figure 2, the process of segment correcting begins with the construction of a K-d tree using the embedding vectors  $f(C(n))$  of all the codewords. When correcting a segment  $\mathbf{t}$ , the segment is firstly mapped to its corresponding deep embedding vector  $\mathbf{u} = f(\mathbf{t})$ . Then, the embedding vector  $\mathbf{u}$  is used to query the K-d tree for its  $k$  nearest neighbors in

the embedding space. Among the retrieved  $k$  nearest neighbors, the codeword with the smallest Levenshtein distance from the segment is identified as the correction.

The tree search of the neighbors of the embedding vector costs  $O(\log |C(n)|)$  in complexity, therefore it is significantly faster than the brute-force search. Nonetheless, it is important to note that the embedded distance is an approximation and could potentially exhibit bias. The correcting of a segment may fail due to such biased embedded distances. Fortunately, this challenge can be addressed by increasing the number  $k$  of queried nearest neighbors. This adjustment costs minimal additional time complexity, as demonstrated in Table 2 and Figure 5. In the subsequent long sequence decoding, we use a value of  $k = 5$  for the segment correcting process.

### 3.4 Depth-first search-based long sequence decoding

Constrained by the biochemical procedures in the DNA storage pipeline, the synthesized DNA molecules usually consist of hundreds of nucleotides. Constructing a code of such length is obviously impractical, and a code capable of correcting only one single edit error throughout the entire DNA sequence lacks application. To generate a long reference, one approach is to concatenate codewords from  $C(n)$  to achieve the desired reference length. However, during the decoding of retrieved read sequences, the segment boundaries can become indiscernible due to synchronization errors. Simply dividing the read into segments of the fixed length  $n$  and applying segment correcting can result in decoding failure. This is because the synchronization mismatch may persist in the subsequent segments following a synchronization error.

To recover segment boundaries from global information, we propose a DFS-based decoding approach. In general, a recursive ternary decoding tree is constructed, as illustrated in Figure 3. Each node of the tree comprises three components: the undecoded sequence, a record of decoded codewords, and a record of distances between decoded segments and their corresponding predicted codewords.

Let  $\mathbf{r}$  be the read sequence. The root node is characterized by the undecoded sequence  $\mathbf{r}$ , an empty record of decoded codewords, and an empty distance record. The left child of the root node contains the undecoded sequence  $\mathbf{r}[n-1:]$ , the decoded codewords record  $[\text{Cr}(\mathbf{r}[n-1])]$ , and the distance record  $[\Delta_L(\text{Cr}(\mathbf{r}[n-1]), \mathbf{r}[n-1])]$ , where  $\text{Cr}(\mathbf{r}[n-1])$  is the segment correction of  $\mathbf{r}[n-1]$ . The middle and right children of the root are similar, but with the replacement of  $n-1$  by  $n$  and  $n+1$  respectively. These three child nodes respectively capture deletion, no error or substitution, and insertion in the first segment. Recursively, the children of a child node are similar by trying to decode the first segments in length  $n-1$ ,  $n$ , and  $n+1$  from the undecoded sequence. Each child node inherits its parent's record lists and appends its new record elements. When the undecoded sequence becomes empty, a node transforms into a leaf node with no children. By comparing the decoded distance records, we select a suitable leaf node as the solution. The decoded codeword record is then concatenated to form the decoded sequence. In this study, we straightforwardly choose the leaf node with the minimum distance records. However, we anticipate that a more in-depth analysis of these distance records could potentially improve the decoding accuracy. In practice, for complexity reduction, we monitor the distance records to terminate the branches with a large distance record in advance. Such branches usually deviate from the error rate of the IDS errors, suggesting a synchronization mismatch in the undecoded sequence.

The code  $C(n)$  is designed to be capable of correcting one edit error in each segment, and maybe failed in correcting multiple edit errors in the same segment. Moreover, the recovery of segment boundaries could also face potential failures. These factors may lead to failures in decoding long sequences, as illustrated in Figure 6 and Table 3. The comparison between metrics of SeqER (resp. SegER) and SeqER\* (resp. SegER\*) in Figure 6 evidently suggests that the primary cause of sequencing errors is the presence of multiple errors within the same segment.

Despite this, the SegER in long sequence decoding remains relatively low and can be overcome effectively by applying an outer RS code with a minimal redundancy of less than 2% ECC symbols, as demonstrated in Figure 7.

### 3.5 Complexity

The encoder of the DoDo-Code operates with time complexity of  $O(1)$ , as the code is pre-generated and encoding merely involves selecting the codeword by index. The segment correcting process incurs a time complexity of at most  $O(n)$  when querying  $k = 1$  neighboring sequence. The set  $A(n)$  containing all sequences of length  $n$  over the 4-ary alphabet has cardinality  $4^n$ , and the code  $C(n)$  is a subset of  $A(n)$  with cardinality less than  $4^n$ . The theoretical query time for the K-d tree is  $O(\log |C(n)|)$ , which is less than  $O(\log 4^n) = O(n)$ . When querying for  $k > 1$  neighbors, the computation of Levenshtein distance increases the time complexity to  $O(n^2)$ . However, since only small  $n$  is concerned in this study, the computation of Levenshtein

distance contributes minimally to the overall time cost. The time required for decoding a long sequence varies depending on different branch termination strategies. If no branch in the ternary tree is allowed, the extra complexity cost by long sequence decoding is  $O(N)$ , where  $N$  represents the number of segments in the sequence. If all branches are allowed, this complexity is increased to  $O(3^{N+1})$ .

### 3.6 Dataset and source code

All the sequences used for training the deep embedding model and testing the DoDo-Code are generated randomly. The groundtruth Levenshtein distance is obtained by a Python module called Levenshtein. Therefore, our source code runs independently of any specific dataset and generates the data on its own. The source code will be made available at <https://github.com/aalennku/DoDo-Code> once this paper is ready for publication.

## References

- [1] G. M. Church, Y. Gao, and S. Kosuri, “Next-generation digital information storage in DNA,” *Science*, vol. 337, no. 6102, pp. 1628–1628, 2012.
- [2] N. Goldman, P. Bertone, S. Chen, C. Dessimoz, E. M. LeProust, B. Sipos, and E. Birney, “Towards practical, high-capacity, low-maintenance information storage in synthesized DNA,” *Nature*, vol. 494, no. 7435, pp. 77–80, 2013.
- [3] R. N. Grass, R. Heckel, M. Puddu, D. Paunescu, and W. J. Stark, “Robust chemical preservation of digital information on DNA in silica with error-correcting codes,” *Angewandte Chemie International Edition*, vol. 54, no. 8, pp. 2552–2555, 2015.
- [4] Y. Erlich and D. Zielinski, “DNA Fountain enables a robust and efficient storage architecture,” *Science*, vol. 355, no. 6328, pp. 950–954, 2017.
- [5] L. Organick, S. D. Ang, Y.-J. Chen, R. Lopez, S. Yekhanin, K. Makarychev, M. Z. Racz, G. Kamath, P. Gopalan, B. Nguyen, *et al.*, “Random access in large-scale DNA data storage,” *Nature biotechnology*, vol. 36, no. 3, pp. 242–248, 2018.
- [6] Y. Dong, F. Sun, Z. Ping, Q. Ouyang, and L. Qian, “DNA storage: research landscape and future prospects,” *National Science Review*, vol. 7, pp. 1092–1107, 01 2020.
- [7] W. Chen, M. Han, J. Zhou, Q. Ge, P. Wang, X. Zhang, S. Zhu, L. Song, and Y. Yuan, “An artificial chromosome for data storage,” *National Science Review*, vol. 8, p. nwab028, 02 2021.
- [8] A. El-Shaikh, M. Welzel, D. Heider, and B. Seeger, “High-scale random access on DNA storage systems,” *NAR Genomics and Bioinformatics*, vol. 4, p. lqab126, 01 2022.
- [9] Z. Ping, D. Ma, X. Huang, S. Chen, L. Liu, F. Guo, S. J. Zhu, and Y. Shen, “Carbon-based archiving: current progress and future prospects of DNA-based data storage,” *GigaScience*, vol. 8, 06 2019. giz075.
- [10] M. Blawat, K. Gaedke, I. Hütter, X.-M. Chen, B. Turczyk, S. Inverso, B. W. Pruitt, and G. M. Church, “Forward error correction for DNA data storage,” *Procedia Computer Science*, vol. 80, pp. 1011 – 1022, 2016. International Conference on Computational Science 2016, ICCS 2016, 6-8 June 2016, San Diego, California, USA.
- [11] A. Lenz, I. Maarouf, L. Welter, A. Wachter-Zeh, E. Rosnes, and A. Graell i Amat, “Concatenated codes for recovery from multiple reads of DNA sequences,” in *2020 IEEE Information Theory Workshop (ITW)*, pp. 1–5, 2021.
- [12] F. Sellers, “Bit loss and gain correction code,” *IRE Transactions on Information theory*, vol. 8, no. 1, pp. 35–38, 1962.
- [13] B. Haeupler and A. Shahrasbi, “Synchronization strings and codes for insertions and deletions—a survey,” *IEEE Transactions on Information Theory*, vol. 67, no. 6, pp. 3190–3206, 2021.
- [14] M. Davey and D. Mackay, “Reliable communication over channels with insertions, deletions, and substitutions,” *IEEE Transactions on Information Theory*, vol. 47, no. 2, pp. 687–698, 2001.

- [15] H. D. Pfister and I. Tal, “Polar codes for channels with insertions, deletions, and substitutions,” in *2021 IEEE International Symposium on Information Theory (ISIT)*, pp. 2554–2559, 2021.
- [16] Z. Yan, C. Liang, and H. Wu, “A segmented-edit error-correcting code with re-synchronization function for DNA-based storage systems,” *IEEE Transactions on Emerging Topics in Computing*, pp. 1–13, 2022.
- [17] M. Welzel, P. M. Schwarz, H. F. Löchel, T. Kabdullayeva, S. Clemens, A. Becker, B. Freisleben, and D. Heider, “DNA-Aeon provides flexible arithmetic coding for constraint adherence and error correction in DNA storage,” *Nature Communications*, vol. 14, no. 1, p. 628, 2023.
- [18] W. H. Press, J. A. Hawkins, S. K. Jones, J. M. Schaub, and I. J. Finkelstein, “HEDGES error-correcting code for DNA storage corrects indels and allows sequence constraints,” *Proceedings of the National Academy of Sciences*, vol. 117, no. 31, pp. 18489–18496, 2020.
- [19] R. R. Varshamov and G. Tenen Holtz, “A code for correcting a single asymmetric error,” *Automatica i Telemekhanika*, vol. 26, no. 2, pp. 288–292, 1965.
- [20] V. I. Levenshtein, “Binary codes capable of correcting deletions, insertions, and reversals,” *Soviet physics. Doklady*, vol. 10, pp. 707–710, 1965.
- [21] L. Calabi and W. Hartnett, “A family of codes for the correction of substitution and synchronization errors,” *IEEE Transactions on Information Theory*, vol. 15, no. 1, pp. 102–106, 1969.
- [22] E. Tanaka and T. Kasai, “Synchronization and substitution error-correcting codes for the levenshtein metric,” *IEEE Transactions on Information Theory*, vol. 22, no. 2, pp. 156–162, 1976.
- [23] K. Cai, Y. M. Chee, R. Gabrys, H. M. Kiah, and T. T. Nguyen, “Correcting a single indel/edit for DNA-based data storage: Linear-time encoders and order-optimality,” *IEEE Transactions on Information Theory*, vol. 67, no. 6, pp. 3438–3451, 2021.
- [24] N. J. Sloane, “On single-deletion-correcting codes,” *Codes and designs*, vol. 10, pp. 273–291, 2000.
- [25] R. Gabrys, V. Guruswami, J. Ribeiro, and K. Wu, “Beyond single-deletion correcting codes: Substitutions and transpositions,” *IEEE Transactions on Information Theory*, vol. 69, no. 1, pp. 169–186, 2023.
- [26] T. Richardson and R. Urbanke, *Modern coding theory*. Cambridge university press, 2008.
- [27] D. Bar-Lev, T. Etzion, and E. Yaakobi, “On the size of balls and anticodes of small diameter under the fixed-length levenshtein metric,” *IEEE Transactions on Information Theory*, vol. 69, no. 4, pp. 2324–2340, 2023.
- [28] G. Wang and Q. Wang, “On the size distribution of levenshtein balls with radius one,” *arXiv preprint arXiv:2204.02201*, 2022.
- [29] W. J. Masek and M. S. Paterson, “A faster algorithm computing string edit distances,” *Journal of Computer and System Sciences*, vol. 20, no. 1, pp. 18–31, 1980.
- [30] A. Backurs and P. Indyk, “Edit distance cannot be computed in strongly subquadratic time (unless SETH is false),” in *Proceedings of the Forty-Seventh Annual ACM Symposium on Theory of Computing, STOC ’15*, (New York, NY, USA), p. 51–58, Association for Computing Machinery, 2015.
- [31] P. Cunningham and S. J. Delany, “K-nearest neighbour classifiers - a tutorial,” *ACM Comput. Surv.*, vol. 54, jul 2021.
- [32] R. Tarjan, “Depth-first search and linear graph algorithms,” *SIAM Journal on Computing*, vol. 1, no. 2, pp. 146–160, 1972.
- [33] R. Ostrovsky and Y. Rabani, “Low distortion embeddings for edit distance,” *J. ACM*, vol. 54, p. 23–es, Oct. 2007.
- [34] D. Chakraborty, E. Goldenberg, and M. Koucký, “Streaming algorithms for embedding and computing edit distance in the low distance regime,” in *Proceedings of the Forty-Eighth Annual ACM Symposium on Theory of Computing, STOC ’16*, (New York, NY, USA), p. 712–725, Association for Computing Machinery, 2016.

- [35] X. Zhang, Y. Yuan, and P. Indyk, “Neural embeddings for nearest neighbor search under edit distance,” 2020.
- [36] X. Dai, X. Yan, K. Zhou, Y. Wang, H. Yang, and J. Cheng, “Convolutional embedding for edit distance,” in *Proceedings of the 43rd International ACM SIGIR conference on research and development in Information Retrieval, SIGIR 2020, Virtual Event, China, July 25-30, 2020*, pp. 599–608, ACM, 2020.
- [37] G. Corso, Z. Ying, M. Pándy, P. Veličković, J. Leskovec, and P. Liò, “Neural distance embeddings for biological sequences,” in *Advances in Neural Information Processing Systems* (M. Ranzato, A. Beygelzimer, Y. Dauphin, P. Liang, and J. W. Vaughan, eds.), vol. 34, pp. 18539–18551, Curran Associates, Inc., 2021.
- [38] A. J. Guo, C. Liang, and Q.-H. Hou, “Deep squared Euclidean approximation to the levenshtein distance for DNA storage,” in *International Conference on Machine Learning*, pp. 8095–8108, PMLR, 2022.
- [39] X. Wei, A. J. Guo, S. Sun, M. Wei, and W. Yu, “Levenshtein distance embedding with poisson regression for dna storage,” *arXiv preprint arXiv:2312.07931*, 2023.
- [40] J. L. Bentley, “Multidimensional binary search trees used for associative searching,” *Communications of the ACM*, vol. 18, no. 9, pp. 509–517, 1975.
- [41] J. H. Friedman, J. L. Bentley, and R. A. Finkel, “An algorithm for finding best matches in logarithmic expected time,” *ACM Transactions on Mathematical Software (TOMS)*, vol. 3, no. 3, pp. 209–226, 1977.
- [42] I. S. Reed and G. Solomon, “Polynomial codes over certain finite fields,” *Journal of the Society for Industrial and Applied Mathematics*, vol. 8, no. 2, pp. 300–304, 1960.
- [43] J. Hadamard, “Sur la distribution des zéros de la fonction  $\zeta(s)$  et ses conséquences arithmétiques,” *Bulletin de la Société mathématique de France*, vol. 24, pp. 199–220, 1896.
- [44] M. Hostetter, “Galois: A performant NumPy extension for Galois fields,” 11 2020.
- [45] A. Krizhevsky, I. Sutskever, and G. E. Hinton, “Imagenet classification with deep convolutional neural networks,” in *Advances in Neural Information Processing Systems 25* (F. Pereira, C. J. C. Burges, L. Bottou, and K. Q. Weinberger, eds.), pp. 1097–1105, Curran Associates, Inc., 2012.
- [46] S. Ioffe and C. Szegedy, “Batch Normalization: Accelerating deep network training by reducing internal covariate shift,” in *International Conference on Machine Learning*, pp. 448–456, PMLR, 2015.
- [47] J. Bromley, I. Guyon, Y. LeCun, E. Säckinger, and R. Shah, “Signature verification using a “Siamese” time delay neural network,” in *Proceedings of the 6th International Conference on Neural Information Processing Systems, NIPS’93*, (San Francisco, CA, USA), p. 737–744, Morgan Kaufmann Publishers Inc., 1993.